Journal of Alloys and Compounds 471 (2009) 44–51

Contents lists available at ScienceDirect

Journal of Alloys and Compounds

journal homepage: www.elsevier.com/locate/jallcom

A study on the non-isothermal transformation kinetics of glassy alloys when the nucleation frequency and crystal growth rate depend on time as a power law
Application to the crystallization of the $Ag_{0.16}As_{0.42}Se_{0.42}$ semiconductor glass

J.L. Cárdenas-Leal, J. Vázquez*, P.L. López-Alemany, P. Villares, R. Jiménez-Garay

Departamento de Física de la Materia Condensada, Facultad de Ciencias, Universidad de Cádiz, Apartado 40, 11510 Puerto Real, Cádiz, Spain

ARTICLE INFO

Article history:
Received 14 February 2008
Received in revised form 11 March 2008
Accepted 11 March 2008
Available online 24 April 2008

PACS:
61.40
64.60.Qb
64.70.Kb
64.70.Pf

Keywords:
Glassy alloy
Glass–crystal transformation
Differential scanning calorimetry
Power law
Kinetic parameters

ABSTRACT

A procedure has been developed to obtain an evolution equation with the temperature for the actual transformed volume fraction under non-isothermal regime and to calculate the kinetic parameters in glassy solids. Once an extended volume of transformed material has been defined and spatially random transformed regions have been assumed, a general expression of the extended volume fraction has been obtained as a function of the temperature, bearing in mind the case presented in the practice of a kinetic exponent with a larger value than 4. This unexpected value is justified assuming that both the nucleation frequency and the crystal growth rate depend on time as a power law. Moreover, considering impingement effect and from the quoted expression, the actual volume fraction transformed has been deduced. The kinetic parameters have been obtained, by assuming that the reaction rate constant is a temperature function of Arrhenius type and using the following considerations: the condition of maximum crystallization rate and the quoted maximum rate. The theoretical model developed and the Johnson–Mehl–Avrami model have been applied to the crystallization kinetics of the $Ag_{0.16}As_{0.42}Se_{0.42}$ glassy alloy, which presents two exothermic peaks. The second peak gives for the kinetic exponent values enough larger than 4 in both models. The quoted values do not fulfil the assumptions of the Avrami model and it is necessary to resort to the hypotheses of the developed model to justify the unexpectedly high value of the kinetic exponent. Moreover, the experimental curve of the transformed fraction shows a better agreement with the theoretical curve of the developed model than with the corresponding curve of the Avrami model, confirming the reliability of the theoretical model developed in order to analyze the transformation kinetics of the above-mentioned glassy alloy.

1. Introduction

Although glass has been used as an artistic medium and industrial material for centuries, it has been only in relatively recent years when the "glass science" has emerged as a field of study in its own right. Yet one of the most active fields of solid-state research in the last decades has been the study of solids that are not crystals, solids in which the arrangement of the atoms lacks the slightest vestige of long-range order.

The advances that have been made in physics and chemistry of these materials, which are known as amorphous solids or non-crystalline, have been widely appreciated within the research community. Solid-state phase transformations play an important role in the production of many materials. Therefore, a great impulse has been given at the study of a general description of the kinetics of phase transformations [1], and accordingly, the last 50 years have seen a theoretical and practical interest in the application of calorimetric analysis techniques to the study of the quoted transformations [2–4]. Thus, the classical theory of nucleation and crystal growth has been developed over the last 60 years. A full development of the theory is given by Christian [5] and a relatively recent review published by Kelton [6].

The calorimetric analysis techniques are very quick and need very small quantities of glass samples to obtain the kinetic parameters of a transformation. There are two thermal analysis regimes: one is the isothermal regime [4–7], in which glass samples are quickly heated up and held at a temperature above glass transition temperature, and the other is so-called non-isothermal regime

* Corresponding author.
E-mail address: jose.vazquez@uca.es (J. Vázquez).

0925-8388/$ – see front matter © 2008 Elsevier B.V. All rights reserved.
doi:10.1016/j.jallcom.2008.03.043

[8–12], in which glass samples are heated up at a fixed heating rate. In general, an isothermal experiment takes longer times than a non-isothermal experiment, but isothermal experimental data can be interpreted by the well-established Johnson–Mehl–Avrami kinetic equation [13–16]. On the contrary, non-isothermal experiments have as an advantage, the rapidity that makes this type of experiments more attractive. The use of non-isothermal techniques to study solid-state transformations and to determine the kinetic parameters of the rate controlling processes has been increasingly widespread. Therefore, the use of the non-isothermal regime has produced a large number of mathematical treatments to analyze thermal process data.

The quoted techniques have become particularly prevalent for the investigation of the processes of nucleation and growth that occur during transformation of the metastable phases in a glassy alloy as it is heated. These techniques provide fast information on such parameters as: glass transition temperature, transformation enthalpy and activation energy over a wide range of temperature [17]. In addition, the physical form and the high thermal conductivity as well as the temperature at which transformations occur in most amorphous alloys make these transformations particularly suited to be analyzed by a differential scanning calorimeter (DSC).

The study of crystallization kinetics in amorphous materials by means of differential scanning calorimetry methods have been widely discussed in the literature [6–18]. There is a large variety of theoretical models and theoretical functions proposed to explain the crystallization kinetics. The application of each of them depends on the type of amorphous material studied and how it has been made.

In the present work, a theoretical procedure has been developed to obtain an evolution equation with temperature for the actual transformed volume fraction. This equation has been obtained bearing in mind the mutual interference of regions growing from separated nuclei and the case in which the kinetic exponent takes a larger value than 4, which is presented in the practice, according to the literature [19]. We justify the quoted case assuming that both the nucleation frequency and the crystal growth rate depend on time as a power law [19–21]. The kinetic parameters and the glass–crystal transformation mechanism have been deduced from DSC experiments, using the above-mentioned equation and assuming a non-isothermal regime.

Moreover, this work applies the theoretical model developed (TMD) and the Johnson–Mehl–Avrami (JMA) model for the analysis of the crystallization kinetics of the $Ag_{0.16}As_{0.42}Se_{0.42}$ glassy semiconductor, which presents two exothermic peaks. The values of the kinetic exponent obtained for the second peak in both models are enough larger than 4. It should be noted that the quoted TMD allows to justify the obtained value, whereas a value of the kinetic exponent cannot be larger than 4, according to JMA model.

Besides, the experimental and theoretical curves of the transformed volume fraction, x, vs. temperature, T have been compared for every model considered. The mentioned curves show a better agreement in the case of the TMD than the curves corresponding to the JMA model, confirming the reliability of the theoretical model developed to describe the glass–crystal transformation of the studied alloy.

2. Theoretical basis

2.1. Nucleation, crystal growth and volume fraction transformed

The theoretical basis to interpret DSC results is provided by the formal theory of transformation kinetics [14–16,22–24]. This formal theory supposes that the crystal growth rate, in general, is anisotropic, and therefore, the volume of a region originating at time $t = (1-\alpha)\tau$ (τ being the nucleation period and where α is a parameter equal to zero in the case of continuous nucleation, and equal to the unit in the case of "site saturation"[25]) is then.

$$\upsilon_\tau = g\prod_i \int_{(1-\alpha)\tau}^{t} u_i(t')\mathrm{d}t' \tag{1}$$

where $u_i(t')$ ($i = 1, 2, 3$) represents the principal growth velocities in the three mutually perpendicular directions, the expression $\prod_i \int_{(1-\alpha)\tau}^{t} u_i(t')\mathrm{d}t'$ condenses the product of the integrals corresponding to the values of the above quoted subscript i and finally g is a geometric factor, which depends on the dimensionality and shape of the crystal growth, and therefore, its dimension equation can be expressed as

$$[g] = [L]^{3-i} \quad ([L] \text{ is the length})$$

Defining an extended volume of transformed material and assuming spatially random transformed regions [26–28], the elemental extended volume fraction, $\mathrm{d}x_e$, in terms of nucleation frequency per unit volume, $I_V(\tau)$, is expressed as

$$\begin{aligned}\mathrm{d}x_e &= [\alpha \mathrm{d}N + (1-\alpha)I_V(\tau)\mathrm{d}\tau]\upsilon_\tau \\ &= g[\alpha dN + (1-\alpha)I_V(\tau)\mathrm{d}\tau]\prod_i \int_{(1-\alpha)\tau}^{t} u_i(t')\mathrm{d}t'\end{aligned} \tag{2}$$

where $\mathrm{d}N$ is the elemental number of nuclei existing per unit volume.

When the crystal growth rate is isotropic, $u_i = u$, an assumption, which is in agreement with the experimental evidence, since in many transformations the reaction product grows approximately as spherical nodules [5], Eq. (2) can be written as

$$\mathrm{d}x_e = g\,[\alpha \mathrm{d}N + (1-\alpha)I_V(\tau)\mathrm{d}\tau]\left[\int_{(1-\alpha)\tau}^{t} u(t')\mathrm{d}t'\right]^m \tag{3}$$

where m is an exponent related to the dimensionality of the crystal growth.

It should be noted that over a sufficiently limited range of temperature (such as the range of transformation peaks in DSC experiments) the quantities $I_V(\tau)$ and $u(t)$ may be considered to have an Arrhenian temperature dependence [28]. In this case, the kinetic exponent is $n = m + 1$ in continuous nucleation processes and $n = m$ in "site saturation" processes. Accordingly, the maximum values of the quoted exponent are 4 and 3, respectively [29]. Nevertheless, in the practice major values are obtained, which according to the literature [30,31] suggest a very high nucleation rate with three-dimensional growth. Besides, these high values of kinetic exponent can be justified in accordance with the literature [19–21] if $I_V(\tau)$ and $u(t)$ depend on time as a power law.

It is interesting to denote that, according to the literature [19], there are two major competing ideas, dating back over 60 years, that try to provide overall models to describe the origin of crystallization textures. The quoted ideas are known as oriented nucleation and oriented growth, and were proposed by Burgers and Louwerse [32] in 1931 and by Barret [33] in 1940, respectively. The essential basis of oriented nucleation is that new grains with the orientation of the major component of the crystallization texture nucleate at a much higher frequency than do grains of all other orientations. In the case of oriented growth, the nuclei already produced with the required orientation for the crystallization grow faster than nuclei of other orientations [19].

With the aim to explain the probable physical nature of the quoted time-dependence for the nucleation frequency and the crys-

tal growth rate, we assume the above-mentioned ideas for the glass–crystal transformation model that will be developed in this work. Thus, it is possible to consider, according to literature [19], that nucleation and crystal growth processes, probably elapse with accelerating rates. Accordingly, theses processes are non-linear and the quantities I_V and u must depend explicitly on time. This dependence can be expressed as a power law in accordance with the literature [19–21]. As it can be observed in Eq. (3), the quoted time-dependence increase the value of the kinetic exponent, a fact that allows to justify unexpectedly high values, larger than 4, which at times are obtained for the quoted exponent in thermal experiments.

Bearing in mind the above-mentioned physical considerations we propose for $I_V(\tau)$ and $u(t)$ the following expressions

$$I_V(\tau) = I_{V0}\tau^p \exp\left(-\frac{E_N}{RT}\right) \tag{4}$$

and

$$u(t) = u_0 t^q \exp\left(-\frac{E_G}{RT}\right) \tag{5}$$

where E_N and E_G are the effective activation energies for nucleation and growth, respectively, p and q are the exponents for each of the quoted power laws and the dimension equations of the coefficients I_{V0} and u_0 can be expressed as

$$[I_{V0}] = [L]^{-3}[T]^{-(p+1)}, \quad [u_0] = [L][T]^{-(q+1)} \quad ([T] \text{ is the time})$$

In the present work, a theoretical method has been developed to integrate Eq. (3) under the quoted conditions, to obtain a general expression for the extended volume fraction, x_e, and to justify high values of kinetic exponent in non-isothermal processes.

Accordingly, assuming a constant heating rate, $\beta = dT/dt$, and considering Eqs. (4) and (5), Eq. (3) becomes

$$dx_e = \frac{gu_0^m}{\beta^{m(q+1)}}\left[\alpha dN + \frac{(1-\alpha)I_{V0}}{\beta^{p+1}}T_\tau^p e^{-E_N/RT_\tau}dT_\tau\right] \times \left(\int_{T_\tau}^{T} T'^q e^{-E_G/RT'}dT'\right)^m \tag{6}$$

T_τ being the temperature corresponding to $(1-\alpha)\tau$ time.

When the case of continuous nucleation, $\alpha = 0$, is considered, the integration of Eq. (6) yields

$$x_e = \frac{gu_0^m I_{V0}}{\beta^{m(q+1)+p+1}}\int_{T_0}^{T} T_\tau^p e^{-E_N/RT_\tau}\left(\int_{T_\tau}^{T} T'^q e^{-E_G/RT'}dT'\right)^m dT_\tau = P_1\int_{T_0}^{T} T_\tau^p e^{-E_N/RT_\tau} I_1^m dT_\tau \tag{7}$$

By the substitution $y' = E_G/RT'$, the integral I_1 of the Eq. (7) is transformed in an exponential integral of order $2+q$, which is a particular case of the order r, which can be expressed, in accordance with the literature [34], by the alternating series

$$S_r(y, y_\tau) = \left[-\frac{e^{-y'}}{y'^r}\sum_{k=0}^{\infty}\frac{(-1)^k(k+r-1)!}{(r-1)!y'^k}\right]_{y_\tau}^{y} \tag{8}$$

Accordingly, taking $r = 2+q$ in Eq. (8), considering that in this type of series the error produced is less than the first term neglected and bearing in mind that in most glass–crystal transformations $y' = E_G/RT' \gg 1$, usually $E_G/RT' \geq 25$ [28], it is possible to use only the first term of the above-mentioned series, without making any appreciable error, and the integral I_1 can be written as

$$I_1 = \frac{R}{E_G}\left[T^{q+2}\exp\left(-\frac{E_G}{RT}\right) - T_\tau^{q+2}\exp\left(-\frac{E_G}{RT_\tau}\right)\right] \tag{9}$$

an expression, which is substituted in Eq. (7) and by means of the expansion of the binomial-potential series [34], one obtains

$$x_e = P_1\left(\frac{R}{E_G}\right)^m\sum_{s=0}^{m}(-1)^s\binom{m}{s}(T^{q+2}e^{-E_G/RT})^{m-s} \times \int_{T_0}^{T} T_\tau^{p+s(q+2)}e^{-(E_N+sE_G)/RT_\tau}dT_\tau = P_1\left(\frac{R}{E_G}\right)^m\sum_{s=0}^{m}(-1)^s\binom{m}{s}(T^{q+2}e^{-E_G/RT})^{m-s}I_2 \tag{10}$$

By the substitution $z_\tau = (E_N + sE_G)/RT_\tau$, the integral I_2 is transformed in an exponential integral of order $p+2+s(q+2)$, which is evaluated as the integral I_1, according to the literature [34], yielding

$$I_2 = \frac{R}{E_N + sE_G}T^{p+2+s(q+2)}\exp\left[\frac{(-E_N + sE_G)}{RT}\right] \tag{11}$$

if it is assumed that $T_0 \ll T$, so that z_0 can be taken as infinity. This assumption is justifiable for any thermal treatment that begins at a temperature where nucleation and crystal growth are negligible, i.e., below the glass transition temperature, T_g, [28]. Substituting Eq. (11) into Eq. (10), introducing the parameter $Q_A = R(R/E_G)^m\sum_{s=0}^{m}[(-1)^s/(E_N + sE_G)]\binom{m}{s}$ and defining a reaction rate constant $K_A = [gI_{V0}u_0^m e^{-(E_N+mE_G)/RT}]^{1/[m(q+1)+p+1]} = K_{A0}e^{-E/RT}$, with an Arrhenian temperature dependence, the extended volume fraction, under non-isothermal regime, is expressed as

$$x_e = Q_A\left(\frac{K_A T^2}{\beta}\right)^n T^{m+1-n} \tag{12}$$

which is a general expression in the case of continuous nucleation processes. It should be noted that E is the overall effective activation energy, K_{A0} the frequency factor with a dimension equation $[T]^{-1}$ ($[T]$ is the time) and the kinetic exponent is written as

$$n = m(q+1) + p + 1 \tag{13}$$

The quoted general expression condenses the four possible cases for a continuous nucleation process under non-isothermal regime, namely: $p \neq 0$, $q \neq 0$; $p = 0$, $q \neq 0$; $p \neq 0$, $q = 0$ and $p = q = 0$.

On the other hand, if the case of "site saturation", $\alpha = 1$, is considered Eq. (6) becomes

$$x_e = \frac{gN_0u_0^m}{\beta^{m(q+1)}}\left[\int_{T_0}^{T} T'^q e^{-E_G/RT'}dT'\right]^m = P_2 I_3^m \tag{14}$$

where N_0 is the number of pre-existing nuclei in the volume of the sample and T_0 is the starting temperature.

By means of a similar calculation process to that of integral I_1, integral I_3 is evaluated, resulting in

$$I_3 = \left(\frac{E_G}{R}\right)^{q+1}\left[\frac{e^{-y'}}{(y')^{q+2}}\right]_{y_0}^{y} = \frac{R}{E_G}T^{q+2}\exp\left(\frac{-E_G}{RT}\right) \tag{15}$$

where the quoted assumption $T_0 \ll T$, so that y_0 can be taken as infinity, is again considered [28].

Substituting Eq. (15) into Eq. (14), introducing the parameter $Q_B = (R/E_G)^m$ and defining a reaction rate constant $K_B =$

$(gN_0u_0^m e^{-mE_G/RT})^{1/m(q+1)} = K_{B0}e^{-E/RT}$, with an Arrhenian temperature dependence, the extended volume fraction, under non-isothermal regime, is expressed as

$$x_e = Q_B\left(\frac{K_B T^2}{\beta}\right)^n T^{m-n} \tag{16}$$

which is a general expression in the case of "site saturation" processes, where K_{B0} is the frequency factor with a dimension equation $[T]^{-1}$ and the kinetic exponent is written as

$$n = m(q+1) \tag{17}$$

The quoted general expression condenses the two possible cases for a "site saturation" process under non-isothermal regime, namely: $q \neq 0$ and $q = 0$.

Bearing in mind the α parameter, already quoted, Eqs. (12) and (16) can be condensed as

$$x_e = Q\left(\frac{KT^2}{\beta}\right)^n T^{m-n+1-\alpha} \tag{18}$$

with the parameter $Q = (R/E_G)^m\{R\sum_{s=0}^{m}[(-1)^s/(E_N + sE_G)]\binom{m}{s}\}^{1-\alpha}$, the reaction rate constant

$K = \left\{gu_0^m N_0^\alpha I_{V0}^{1-\alpha} e^{-[(1-\alpha)E_N + mE_G]/RT}\right\}^{1/n} = K_0 e^{-E/RT}$ and the kinetic exponent is given as

$$n = m(q+1) + (1-\alpha)(p+1) \tag{19}$$

It should be noted that Eq. (18) is a general expression for the extended volume fraction, when non-isothermal treatments are performed, both for continuous nucleation and for "site saturation" processes.

By using the explicit form of Arrhenian temperature dependence for the reaction rate constant Eq. (18) can be rewritten as

$$x_e = QK_0^n\left(\frac{T^2}{\beta}\right)^n\left(\frac{nE}{R}\right)^{m-n+1-\alpha}\left[\left(\frac{RT}{nE}\right)^{m-n+1-\alpha}\exp\left(-\frac{nE}{RT}\right)\right] \tag{20}$$

Given that, asymptotically, for $nE \gg RT$ the exponential term in Eq. (20) changes much faster compared to the power law, in square brackets, the latter can be treated almost as a constant, in accordance with the literature [24], and then Eq. (20) becomes

$$x_e = D\left(\frac{T^2}{\beta}\right)^n \exp\left(-\frac{nE}{RT}\right) \tag{21}$$

where D can be considered as a constant, with a dimension equation $[\theta T]^{-n}$ ($[\theta]$ is the temperature).

On the other hand, it is well known the impingement effect in the glass–crystal transformations. In accordance with the literature [5], to obtain a general kinetic equation for the actual transformed volume fraction, the mutual interference of regions growing from separated nuclei must be considered. When two such regions impinge on each other it is possible that the two regions develop a common interface, over which growth ceases, although it continues normally elsewhere. In this sense, following the literature [5,35] and considering the hypothesis of random nucleation it is possible to write the relationship between the actual volume, V_b, and the extended volume, V_e, in the form

$$dV_b = \left(1 - \frac{V_b}{V}\right)^{\gamma_i} dV_e = (1-x)^{\gamma_i} dV_e \tag{22}$$

where $x = V_b/V$ is the actual transformed volume fraction, V is the volume of the whole assembly, γ_i is termed the impingement exponent, and considering $dV_e = V dx_e$, Eq. (22) can be expressed as

$$(1-x)^{-\gamma_i} dx = dx_e \tag{23}$$

Defining an impingement factor $\delta_i = (\gamma_i - 1)^{-1}$, the general solution of the preceding differential equation is given as

$$x = 1 - (1 + x_e\delta_i^{-1})^{-\delta_i} \tag{24}$$

By substituting Eq. (21) into Eq. (24), one obtains

$$x = 1 - \left[1 + \frac{1}{\delta_i} D\left(\frac{T^2}{\beta}\right)^n \exp\left(-\frac{nE}{RT}\right)\right]^{-\delta_i} \tag{25}$$

an equation for the actual transformed volume fraction corresponding to the above-developed model.

It should be noted that if the impingement exponent, $\gamma_i = 1$, $\delta_i \to \infty$, and considering Eq. (21) Eq. (24) becomes

$$x = 1 - \lim_{\delta_i \to \infty}\left[1 + \left(\frac{\delta_i}{x_e}\right)^{-1}\right]^{-\delta_i}$$

$$= 1 - \exp(-x_e) = 1 - \exp\left[-D\left(\frac{T^2}{\beta}\right)^n \exp\left(-\frac{nE}{RT}\right)\right] \tag{26}$$

corresponding to the JMA model.

In the following section, we will be deducing that the values of the constant D and the kinetic exponent are different for each model, whereas the value of the activation energy is the same in both models.

2.2. Calculating the kinetics parameters

It is well known that between the proposed methods in the literature [28] to analyze the crystallization kinetics in glass-forming liquids the differential methods play an important role. From this point of view, the crystallization rate is obtained in this work, taking the derivative of the actual crystallized volume fraction [Eq. (24)] with respect to time, resulting in

$$\frac{dx}{dt} = (1 + x_e\delta_i^{-1})^{-(\delta_i+1)}\frac{dx_e}{dt} \tag{27}$$

The maximum crystallization rate is found making $d^2x/dt^2 = 0$, yielding

$$\left.\frac{d^2x_e}{dt^2}\right|_p = \left(\frac{\delta_i + 1}{\delta_i}\right)(1 + x_e|_p\delta_i^{-1})^{-1}\left.\left(\frac{dx_e}{dt}\right)^2\right|_p \tag{28}$$

where the subscript p denotes the quantity values corresponding to the maximum crystallization rate.

Taking the first and the second derivative of the extended volume fraction [Eq. (21)] with respect to time, substituting both into Eq. (28), and dividing the resulting equation by expression $Dn\beta^{2-n}T_p^{2n-2}\exp(-nE/RT_p)$, and finally extracting common factor n in the left hand side, the quoted Eq. (28) can be rewritten as

$$n\left(2 + \frac{E}{RT_p}\right)^2 - 2\left(1 + \frac{E}{RT_p}\right) = n\left(2 + \frac{E}{RT_p}\right)^2 D\left(\frac{T_p^2}{\beta}\right)^n e^{-nE/RT_p} \times \left(\frac{\delta_i + 1}{\delta_i}\right)(1 + x_e|_p\delta_i^{-1})^{-1} \tag{29}$$

and dividing by expression $n(2 + E/RT_p)^2$, Eq. (29) becomes

$$\left(\frac{\delta_i + 1}{\delta_i}\right)(1 + x_e|_p\delta_i^{-1})^{-1} D\left(\frac{T_p^2}{\beta}\right)^n e^{-nE/RT_p} = 1 - \frac{2}{n}\frac{(1 + E/RT_p)}{(2 + E/RT_p)^2} \tag{30}$$

which relates the crystallization kinetics parameters E, n and δ_i to the quantity values that can be determined experimentally, and

which correspond to the maximum crystallization rate. Bearing in mind Eq. (21) and that in most transformation reactions $E/RT_p \gg 1$ (usually $E/RT_p \geq 25$), an assumption already quoted, Eq. (30) yields

$$\left(\frac{\delta_i + 1}{\delta_i}\right)(1 + \delta_i^{-1} x_e|_p)^{-1} x_e|_p = 1 \tag{31}$$

Substituting in Eq. (31) the expression $x_e|_p$ taken from Eq. (24) and by making explicit the quantity $1 - x_p$, one obtains

$$1 - x_p = \left(\frac{\delta_i}{\delta_i + 1}\right)^{\delta_i} \tag{32}$$

an expression from which, the impingement factor, δ_i, can be evaluated in a set of exotherms taken at different heating rates, by using a method of successive approximations (e.g. secant method). The corresponding mean value may be taken as the most probable value of the impingement factor in the glass–crystal transformation process.

Substituting in Eq. (31) the expression $(1 + \delta_i^{-1} x_e|_p)^{-1}$ taken from Eq. (24), bearing in mind Eq. (32) yields $x_e|_p = 1$, and then the logarithmic form of Eq. (21) is expressed as

$$\ln \frac{T_p^2}{\beta} = \frac{E}{RT_p} - \ln h \tag{33}$$

which is a linear function, whose slope and intercept give the overall effective activation energy, E, and the quantity $h = D^{1/n}$ [see Eqs. (20) and (21)], which is related to the probability of effective collisions for the formation of the activated complex.

Besides, substituting in Eq. (27) for the maximum crystallization rate, the expression $(1 + \delta_i^{-1} x_e|_p)^{-(\delta_i+1)}$ and $(dx_e/dt)|_p$ taken from Eqs. (24) and (21), bearing in mind that $x_e|_p = 1$ and considering the above quoted assumption $E/RT_p \gg 1$, one obtains

$$n = RT_p^2 \left.\frac{dx}{dt}\right|_p [(1 - x_p)^{(\delta_i+1)/\delta_i} \beta E]^{-1} \tag{34}$$

an expression which allows the kinetic exponent, n, to be calculated in a set of exotherms taken at different heating rates. The corresponding mean value may be considered as the most probable value of the kinetic exponent of the transformation process.

The constant D can be evaluated from the quantity h, already quoted, Eq. (33), and the kinetic exponent, n. It should be noted that the quoted constant is related to frequency factor, K_0, of the glass–crystal transformation process, according to Eqs. (20) and (21).

It is important to mark that in JMA model, where it is assumed that I_v and u do not depend explicitly on the time ($p = q = 0$), $n = m + 1 - \alpha$, according to Eq. (19), and $h = D^{1/n} = Q^{1/n} K_0$ in Eq. (33) [see Eqs. (20) and (21)]. Besides, considering Eq. (32), and Eq. (34) becomes

$$n = RT_p^2 \left.\frac{dx}{dt}\right|_p (0.37 \beta E)^{-1} \tag{35}$$

an expression which allows the kinetic exponent, n, to be calculated in the quoted model.

3. Experimental

The $Ag_{0.16}As_{0.42}Se_{0.42}$ glassy semiconductor was prepared in bulk form by the standard melt quenching method. High-purity (99.999%) silver, arsenic and selenium in appropriate atomic percentage proportions were weighed and introduced into a quartz glass ampoule (6 mm diameter). The content of the ampoule (7 g per batch) was sealed at a pressure of 10^{-2} Pa and heated in a rotating furnace at around 1125 K for 120 h and submitted to a longitudinal rotation of 1/3 rpm in order to ensure the homogeneity of the molten material. It was then immersed in a receptacle containing water with ice in order to solidify the material quickly, avoiding the crystallization of the compound.

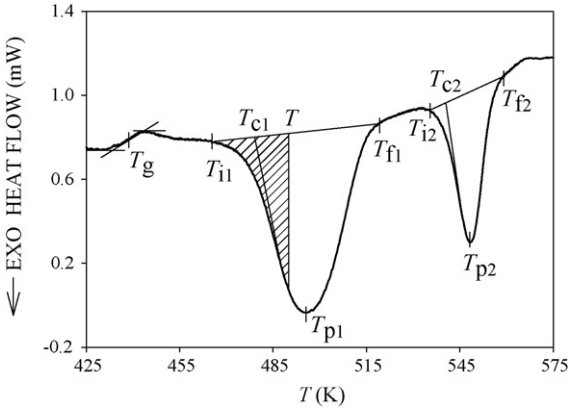

Fig. 1. Typical DSC trace of $Ag_{0.16}As_{0.42}Se_{0.42}$ semiconductor alloy at a heating rate of 16 K min^{-1}. The hatched area shows A_T, the area between T_i and T.

The amorphous state of the material was checked through a diffractometric X-ray scan, in a Bruker AXS, D8 Advance model diffractometer. The homogeneity and composition of the sample were verified through scanning electron microscopy (SEM) in a JEOL, scanning microscope JSM 820. The thermal behaviour was investigated using a Perkin-Elmer DSC7 differential scanning calorimeter with an accuracy of ±0.1 K. Temperature and energy calibrations of the instrument were performed, for each heating rate, using the well-known melting temperatures and melting enthalpies of high-purity zinc and indium supplied with the instrument [36].

The samples weighing about 10 mg were crimped in aluminium pans, and scanned from room temperature through their glass transition temperature, T_g, at different heating rates of 2, 4, 8, 16, 32 and 64 K min^{-1}. An empty aluminium pan was used as reference, and in all cases a constant 60 ml min^{-1} flow of nitrogen was maintained in order to provide a constant thermal blanket within the DSC cell, thus eliminating thermal gradients and ensuring the validity of the applied calibration standard from sample to sample. The glass transition temperature, T_g, was considered as a temperature corresponding to the inflection of the lambda-like trace on the DSC scan, as shown in Fig. 1.

The crystallized fraction, x, corresponding to an exothermic peak at any temperature, T, is given by $x = A_T/A$, where A is the total area limited by the exotherm of the quoted peak between the temperature, T_i, where the crystallization just begins and the temperature, T_f, where the crystallization is completed and A_T is the area between the initial temperature and a generic temperature T, see Fig. 1.

4. Results

The typical DSC trace of $Ag_{0.16}As_{0.42}Se_{0.42}$ semiconductor glass obtained at a heating rate of 16 K min^{-1} and plotted in Fig. 1 shows two exothermic peaks clearly separated. Both peaks exhibit two characteristic phenomena, which are resolved in the temperature region studied. The first one corresponds to the extrapolated onset crystallization temperature, T_c, (T_{c1} = 478.3 K for the first peak and T_{c2} = 539.8 K for the second peak) and the last one to the peak temperature of crystallization, T_p, (T_{p1} = 495.4 K for the first peak and T_{p2} = 548.4 K for the second peak), of the above-mentioned semiconductor glass. The quoted DSC trace shows the typical behaviour of a glass–crystal transformation. The data of the thermograms for the different heating rates, β, quoted in Section 3, show values of the quantities T_c and T_p, which increase with increasing β for both peaks, a property, which has been reported in the literature [37].

Table 1
Characteristic temperatures and enthalpies of the crystallization process of the $Ag_{0.16}As_{0.42}Se_{0.42}$ glassy alloy

Parameter	Experimental value	
	First peak	Second peak
T_i (K)	459.9–476.5	508.5–553.8
T_p (K)	481.2–508.5	515.3–578.0
ΔT (K)	37.6–62.4	16.6–38.6
ΔH (mcal mg^{-1})	4.2–8.2	1.4–4.0

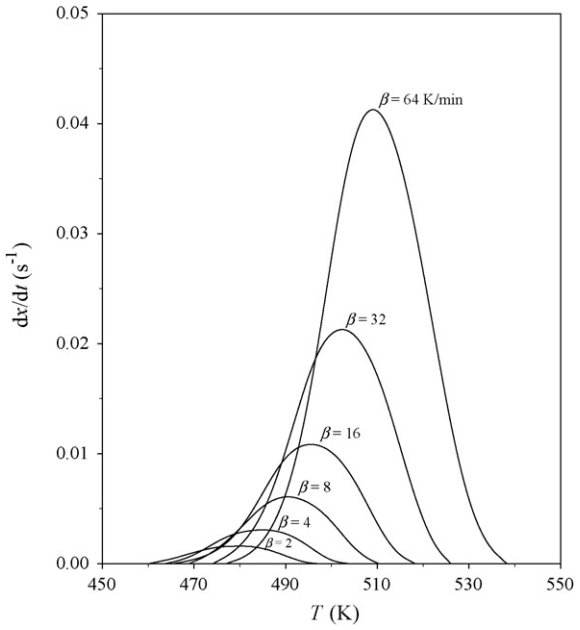

Fig. 2. Crystallization rate vs. temperature for the first exothermal peak at different heating rates.

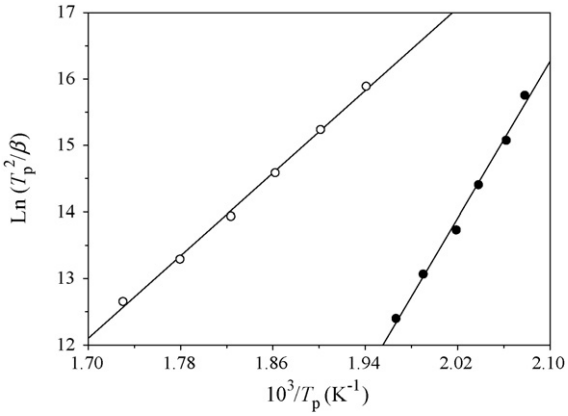

Fig. 3. Experimental plots of $\ln(T_p^2/\beta)$ vs. $1/T_p$ and straight regression lines of the $Ag_{0.16}As_{0.42}Se_{0.42}$ alloy (β in K s^{-1}): (●) first peak; (○) second peak.

4.1. Glass–crystal transformation

The kinetics analysis of the crystallization reactions is related to the knowledge of the reaction rate constant as a function of the temperature. In this sense, a great number of analytical methods, proposed in the literature to describe the above-mentioned reactions, assume that the reaction rate constant can be represented by means of an Arrhenius type temperature dependence [28,38]. This assumption involves that the maximum values of the kinetic exponent are 4 and 3 in continuous nucleation and in "site saturation" processes, respectively [29]. Nevertheless, in the practice major values of the quoted exponent are obtained, which according to the literature [30,31] suggest a very high nucleation rate with three-dimensional growth. Bearing in mind this assumption we analyze the glass–crystal transformation kinetics of $Ag_{0.16}As_{0.42}Se_{0.42}$ alloy in accordance with the theory developed in Section 2.

With the aim to analyze the crystallization kinetics of the above-mentioned alloy, the variation intervals of the quantities described by the thermograms for the different heating rates, quoted in Section 3, and corresponding to the two peaks of crystallization, are obtained and given in Table 1, where T_i and T_p are the temperatures at which crystallization begins and that corresponding to the maximum crystallization rate, respectively, and ΔT is the width of each crystallization peak. The crystallization enthalpy ΔH is also determined for each of the heating rates.

The limited area by each peak of the DSC curve is directly proportional to the total amount of crystallized alloy. The ratio between the ordinates of the exotherm and the total area of a peak gives the corresponding crystallization rates, which make it possible to plot the curves dx/dt vs. T for the different heating rates. As an illustrative example, the quoted curves corresponding to the first peak of alloy studied are represented in Fig. 2. It should be noted that the $(dx/dt)|_p$ values increase in the same proportion that the heating rate, a property which has been widely discussed in the literature [39].

From the experimental data the plots of $\ln(T_p^2/\beta)$ vs. $1/T_p$ at each heating rate have been drawn and also the straight regression line (SRL) shown in Fig. 3 for each one of the peaks of the quoted alloy. From the slopes and intercepts of these experimental lines, according to Eq. (33), both the overall effective activation energy, E, and the quantity h are obtained for each peak of the glass–crystal transformation, which, together with the SRL equations, are presented in Table 2. Moreover, the experimental data $(dx/dt)|_p$, T_p and x_p, shown in Table 3, allow to obtain for each peak of crystallization the parameters δ_i and n for TMD and the parameter n for JMA model.

For the first model, by using Eq. (32) and following the secant method of successive approximations, the impingement factor has been evaluated for each heating rate and for the two peaks obtained. The calculation of the kinetic exponent has been carried out for each heating rate, by using Eq. (34), from the quoted experimental data, together with the value of the activation energy, given in Table 2 for each peak, and the corresponding results of the impingement factor. The values both for δ_i and for n are also given in Table 3. Bearing in mind that the calorimetric analysis is an indirect method which only makes it possible to obtain mean values for the parameters which control the mechanism of a reaction, δ_i and n, the mentioned mean values have been calculated and given in Table 3. For the second model, the kinetic exponent has been calculated in the same way but using Eq. (35). The values obtained and the corresponding mean value for each peak are also given in Table 3.

We have examined the mean values of the kinetic exponent for every peak according to the JMA model and we find a value $\langle n \rangle = 0.98$ for the first peak, which fulfils suitably the assumptions of the quoted model, whereas the second peak gives an unexpectedly high value of the kinetic exponent, $\langle n \rangle = 5.32$. This last value is not in agreement with the assumptions of the JMA model, since for a constant rate of growth, u, of new grains and a constant rate of their nucleation, I_v, the expected value of the kinetic exponent will be 4 falling 3 if all new grains nucleate at the start of the glass–crystal transformation, giving "site saturation" [25,40].

Bearing in mind this fact we have considered the TMD, where both I_v and u depend on time as a power law [19–21] of which exponents are p and q, respectively [see Eqs. (4) and (5)]. For the model lately quoted Eq. (19) is obtained, where the kinetic exponent

Table 2
Straight regression lines (SRL) fitted to values of the $\ln(T_p^2/\beta)$ and kinetic parameters of the two peaks analyzed

Peak	SRL	E (kcal mol^{-1})	h (K s)$^{-1}$	r
First	$29.4607 \times 10^3/T_p - 45.6028$	58.92	6.38×10^{19}	0.9969
Second	$15.5240 \times 10^3/T_p - 14.2902$	31.05	1.61×10^6	0.9986

r is the correlation coefficient.

Table 3
Maximum crystallization rate, corresponding temperature and crystallized volume fraction, kinetic exponent and impingement factor for the different heating rates and for the two exothermic peaks

Peak	β (K min^{-1})	$10^3(dx/dt)\|_p$ (s^{-1})	T_p (K)	x_p	TMD					JMA		
					δ_i	n	$\langle\delta_i\rangle$	$\langle n\rangle$	D (K s)$^{-n}$	n	$\langle n\rangle$	D (K s)$^{-n}$
First	2	1.70	481.2	0.5512	1.8724	1.37				1.08		
	4	3.12	485.0	0.5392	1.5802	1.32				1.01		
	8	6.27	490.7	0.5117	1.1349	1.48	1.2231	1.41	8.41×10^{27}	1.04	0.98	2.56×10^{19}
	16	10.92	495.4	0.5022	1.0240	1.35				0.92		
	32	21.06	502.5	0.5066	1.0729	1.33				0.92		
	64	41.69	508.5	0.4545	0.6540	1.59				0.93		
Second	2	4.16	515.3	0.5384	1.5626	7.58				5.77		
	4	7.28	526.0	0.5665	2.3973	6.36				5.26		
	8	14.46	537.1	0.5536	1.9405	6.84	1.8969	6.74	6.82×10^{41}	5.45	5.32	1.05×10^{33}
	16	26.55	548.4	0.5409	1.6165	6.80				5.21		
	32	50.00	562.0	0.5545	1.9697	6.45				5.16		
	64	93.42	578.0	0.5520	1.8947	6.43				5.09		

Table 4
Theoretical expressions of the transformed volume fraction for the JMA model and for the TMD when $\beta = 4$ K min^{-1}

Model	Peak	Equation
JMA	1	$x = 1 - \exp[-3.64 \times 10^{20} T^{1.96} \exp(-28870.8/T)]$
	2	$x = 1 - \exp[-1.90 \times 10^{39} T^{10.64} \exp(-82593.0/T)]$
TMD	1	$x = 1 - [1 + 3.11 \times 10^{29} T^{2.82} \exp(-41538.6/T)]^{-1.2331}$
	2	$x = 1 - [1 + 3.04 \times 10^{49} T^{13.48} \exp(-104638.5/T)]^{-1.8969}$

is a function of p and q, that allows to justify the high value of the quoted exponent calculated for the second peak.

It should be noted that the constant D, given in Table 3, has been calculated for each peak in both models from the corresponding values of h and $\langle n\rangle$ using the relationship $h = D^{1/n}$, already quoted in Section 2.2.

Considering Eqs. (25) and (26), corresponding to the two quoted models, the expressions of the theoretical transformed fraction, x, as functions of the temperature, are obtained and given in Table 4 for $\beta = 4$ K min^{-1} and for every peak. As an illustrative example, which confirms the validity of the TMD, we represent in Fig. 4 the experimental and theoretical curves x vs. T. In this figure, it is observed a satisfactory agreement between the experimental curve and the theoretical curve of each model considered. This agreement is better enough for the TMD than for the JMA model, specially in the second peak, where the kinetic exponent has an unexpectedly high value, which is not in agreement with the assumptions of the JMA model.

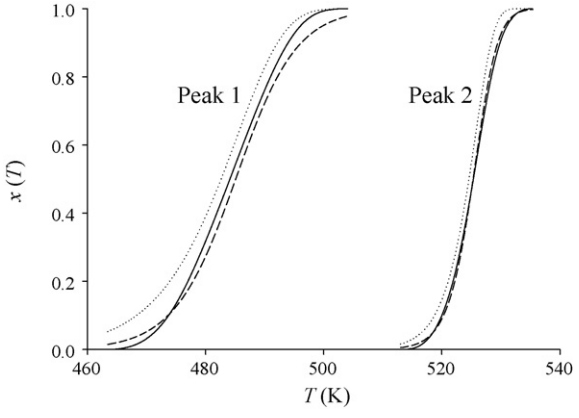

Fig. 4. Transformed volume fraction vs. temperature for the two exothermal peaks at heating rate of 4 K min^{-1}: (—) experimental data; (···) JMA model; (– –) TMD.

5. Conclusions

The theoretical method developed enables us to study the evolution with temperature of the actual transformed volume fraction and to analyze the glass–crystal transformation mechanisms in solid systems. This method assumes the concept of extended volume of the transformed material and the condition of randomly located nuclei, together with the supposition of mutual interference of regions growing from separated nuclei and the case of which the kinetic exponent takes a value larger than 4. To analyze the quoted case, we propose that both the nucleation frequency and the crystal growth rate depend on time as a power law. By using these assumptions, we have obtained a general expression for the actual transformed volume fraction, as a function of the temperature in non-isothermal crystallization processes. It should be noted that the quoted power law allows to justify unexpectedly high values for the kinetic exponent.

The kinetic parameters have been deduced by using the following considerations: the condition of maximum crystallization rate and the quoted maximum rate. The theoretical method developed has been applied to the experimental data corresponding to the crystallization kinetics of the $Ag_{0.16}As_{0.42}Se_{0.42}$ glassy alloy, which presents two exothermic peaks. The mean values of the kinetic exponent obtained for the second peak are $\langle n\rangle = 5.32$ and $\langle n\rangle = 6.74$ in the JMA model and in the TMD, respectively. The first one does not fulfil the assumptions of the corresponding model, whereas the second one is justified by means of TMD's hypotheses. Moreover, the experimental and theoretical curves x vs. T show that the TMD is more of agreement with the experimental data than JMA model. These considerations allow to confirm the reliability of the theoretical model developed in order to analyze the transformation kinetics of the studied alloy.

Acknowledgements

The authors are grateful to the Junta de Andalucia (PAI/EXCEL//FQM0654) and the Spanish Ministry of Science and Education (MEC) (project no. FIS 2005-1409) for their financial supports.

References

[1] A.T.W. Kempen, F. Sommer, E.J. Mittemeijer, J. Mater. Sci. 37 (2002) 1321.
[2] V.I. Tkatch, A.I. Limanovski, V.Y. Kameneva, J. Mater. Sci. 32 (1997) 5669.
[3] S.H. Hong, G.L. Messing, J. Am. Ceram. Soc. 80 (1997) 1551.
[4] J.Q. Zhu, Z.L. Bo, D.K. Dong, Phys. Chem. Glasses 37 (1996) 264.
[5] J.W. Christian, The Theory of Transformations in Metals and Alloys, second ed., Pergamon Press, New York, 1975.

[6] K.F. Kelton, Crystal Nucleation in Liquids and Glasses, in: Solid State Physics, vol. 45, Academic Press, New York, 1991.
[7] M.A. Abdel-Rahim, M.M. Ibrahim, M. Dongol, A. Gaber, J. Mater. Sci. 27 (1992) 4685.
[8] J. Vázquez, R. González-Palma, P.L. López-Alemany, P. Villares, R. Jiménez-Garay, J. Phys. Chem. Solids 68 (2007) 855.
[9] M.C. Weinberg, R. Kapral, J. Chem. Phys. 91 (1989) 7146.
[10] J.R. Frade, J. Am. Ceram. Soc. 81 (1998) 2654.
[11] C.S. Ray, X. Fang, D.E. Day, J. Am. Ceram. Soc. 83 (2000) 865.
[12] P.L. López-Alemany, J. Vázquez, P. Villares, R. Jiménez-Garay, Mater. Lett. 57 (2003) 2722.
[13] W.A. Johnson, K.F. Mehl, Trans. Am. Inst. Mining, Met. Eng. 135 (1939) 416.
[14] M. Avrami, J. Chem. Phys. 7 (1939) 1103.
[15] M. Avrami, J. Chem. Phys. 8 (1940) 212.
[16] M. Avrami, J. Chem. Phys. 9 (1941) 177.
[17] Z. Altounian, J.O. Strom-Olsen, in: R.D. Shull, A. Joshi (Eds.), Thermal Analysis in Metallurgy, Warrendale, PA, 1992, p. 155.
[18] H.E. Kissinger, Anal. Chem. 29 (1957) 1702.
[19] R.D. Doherty, K. Kashyap, S. Panchanadeeswaran, Acta Metall. Mater. 41 (1993) 3029.
[20] W.B. Hutchinson, S. Jonsson, L. Ryde, Scripta Metall. 23 (1989) 671.
[21] C. Necker, R.D. Doherty, A.D. Rollet, in: Proceedings of the 9th International Conference on Textures, Avignon, France, 1990, Tex. Microstruct. 14-18 (1991) 635.
[22] D.W. Henderson, J. Non-Cryst. Solids 30 (1979) 301.
[23] A.N. Kolomogorov, Bull. Acad. Sci. USSR (Sci. Mater. Nat.) 3 (1937) 3551.
[24] P.L. López-Alemany, J. Vázquez, P. Villares, R. Jiménez-Garay, J. Non-Cryst. Solids 274 (2000) 249.
[25] J.W. Cahn, Acta Metall. 4 (1956) 572, Acta Metall. 4 (1956) 449.
[26] J. Vázquez, P. Villares, R. Jiménez-Garay, J. Alloys. Compd. 257 (1997)259.
[27] V.A. Shneidman, D.R. Uhlmann, J. Chem. Phys. 109 (1998) 186.
[28] H. Yinnon, D.R. Uhlmann, J. Non-Cryst. Solids 54 (1983) 253.
[29] Y. He, G.M. Dougherty, G.J. Shiflet, S.J. Poon, Acta Mater. 41 (1993) 337.
[30] F. Ye, K. Lu, J. Non-Cryst. Solids 262 (2000) 228.
[31] R. Jain, D. Bhandari, N.S. Saxena, S.K. Sharma, A. Tripathi, Bull. Mater. Sci. 24 (2001) 27.
[32] W.G. Burgers, P.C. Louwerse, Z. Physik 61 (1931) 605.
[33] C.S. Barret, Trans. Am. Soc. Met. 137 (1940) 128.
[34] J. Vázquez, C. Wagner, P. Villares, R. Jiménez-Garay, Acta Mater. 44 (1996) 4807.
[35] J. Vázquez, R. González-Palma, P.L. López-Alemany, P. Villares, R. Jiménez-Garay, J. Phys. Chem. Solids 66 (2005) 1264.
[36] Perkin Elmer, PC Series, Thermal Analysis System, DSC7 Differential Scanning Calorimeter, Operator's Manual, Norwalk, Connecticut, 1989.
[37] J. Vázquez, P.L. López-Alemany, P. Villares, R. Jiménez-Garay, Mater. Chem. Phys. 57 (1998) 162.
[38] S.O. Kasap, C. Juhasz, J. Chem. Soc., Farady Trans. 2 (81) (1985) 811.
[39] P.L. López-Alemany, J. Vázquez, P. Villares, R. Jiménez-Garay, J. Alloys. Compd. 285 (1999) 185.
[40] A.D. Rollet, R.D. Doherty, D.J. Srolovitz, M.P. Anderson, Acta Metall. 37 (1989) 627.